



## Open Archive Toulouse Archive Ouverte (OATAO)

OATAO is an open access repository that collects the work of Toulouse researchers and makes it freely available over the web where possible.

This is an author-deposited version published in: <http://oatao.univ-toulouse.fr/>  
Eprints ID: 8699

DOI:10.1021/la304278n

Official URL: <http://dx.doi.org/10.1021/la304278n>

**To cite this version:**

Bédier, Amélie and Seichepine, Florent and Flahaut, Emmanuel and Loubinoux, Isabelle and Vaysse, Laurence and Vieu, Christophe *Elucidation of the Role of Carbon Nanotube Patterns on the Development of Cultured Neuronal Cells*. (2012) Langmuir, vol. 28 (n° 50). pp. 17363-17371. ISSN 0743-7463

Any correspondence concerning this service should be sent to the repository administrator:  
[staff-oatao@inp-toulouse.fr](mailto:staff-oatao@inp-toulouse.fr)

# Elucidation of the Role of Carbon Nanotube Patterns on the Development of Cultured Neuronal Cells

Amélie Bédier,<sup>\*,†,‡,||</sup> Florent Seichepine,<sup>†,⊥,@,#</sup> Emmanuel Flahaut,<sup>†,⊥,@,#</sup> Isabelle Loubinoux,<sup>∇,○</sup> Laurence Vaysse,<sup>∇,○</sup> and Christophe Vieu<sup>†,§,||</sup>

<sup>†</sup>CNRS-LAAS, 7 avenue du colonel Roche, F-31400 Toulouse, France

<sup>‡</sup>Université de Toulouse, UPS, LAAS F-31400 Toulouse, France

<sup>§</sup>Université de Toulouse, INSA, LAAS F-31400 Toulouse, France

<sup>||</sup>ITAV, Centre Pierre Potier, F-31106 Toulouse, France

<sup>⊥</sup>Université de Toulouse, LAAS F-31400 Toulouse, France

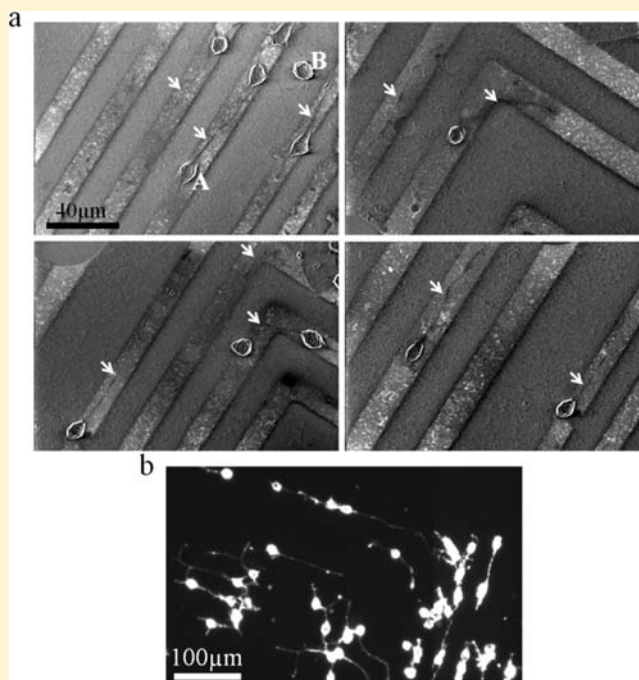
<sup>@</sup>Université de Toulouse; UPS, INP; Institut Carnot Cirimat; 118, route de Narbonne, F-31062 Toulouse Cedex 9, France

<sup>#</sup>CNRS; Institut Carnot Cirimat; F-31062 Toulouse, France

<sup>∇</sup>INSERM, Imagerie Cérébrale et Handicaps Neurologiques UMR 825; F-31059 Toulouse, France

<sup>○</sup>Université de Toulouse, UPS, Imagerie Cérébrale et Handicaps Neurologiques UMR 825, CHU Purpan, F-31059 Toulouse, France

**ABSTRACT:** Carbon nanotubes (CNTs) promise various novel neural biomedical applications for interfacing neurons with electronic devices or to design appropriate biomaterials for tissue regeneration. In this study, we use a new methodology to pattern SiO<sub>2</sub> cell culture surfaces with double-walled carbon nanotubes (DWNTs). In contrast to homogeneous surfaces, patterned surfaces allow us to investigate new phenomena about the interactions between neural cells and CNTs. Our results demonstrate that thin layers of DWNTs can serve as effective substrates for neural cell culture. Growing neurons sense the physical and chemical properties of the local substrate in a contact-dependent manner and retrieve essential guidance cues. Cells exhibit comparable adhesion and differentiation scores on homogeneous CNT layers and on a homogeneous control SiO<sub>2</sub> surface. Conversely, on patterned surfaces, it is found that cells preferentially grow on CNT patterns and that neurites are guided by micrometric CNT patterns. To further elucidate this observation, we investigate the interactions between CNTs and proteins that are contained in the cell culture medium by using quartz crystal microbalance measurements. Finally, we show that protein adsorption is enhanced on CNT features and that this effect is thickness dependent. CNTs seem to act as a sponge for culture medium elements, possibly explaining the selectivity in cell growth localization and differentiation.



## 1. INTRODUCTION

Carbon Nanotubes (CNTs) have different properties, such as extraordinary strength, toughness, electrical conductivity, and specific surface area, which make them excellent candidates for interfacing with neural systems for the development of biocompatible, durable, and robust neuroprosthetic devices. CNTs have been studied as possible substrates for neuronal cell adhesion.<sup>1,2</sup> Studies have demonstrated that CNT surfaces act as an extremely efficient biocompatible substrate on which

neurons adhere and proliferate. CNT homogeneous films have also been shown to influence neurite branching, length, and density.<sup>3,4</sup> In vivo, CNTs have been very recently investigated as scaffold for stem cell therapy because of their favorable electrical properties, and it has been shown that CNTs could reduce the size of a damaged brain area of a rat.<sup>5</sup> In addition to

being biocompatible,<sup>2,3,6,7</sup> CNTs are electrically conducting (they can behave like a metal or like a semiconductor, depending on their structure) and can be integrated into microfabricated devices. This panel of properties opens up new and exciting prospects. A recent development in CNT-based devices is represented by the design of multi-electrode arrays (MEA) to both electrically stimulate and record signals from neurons. Such MEAs were made by synthesizing islands of CNTs on lithographically defined, conductive substrates. Reports indicate the possibility of directly stimulating isolated neurons via CNTs in culture.<sup>4,8</sup> It was also demonstrated that coating of metal electrodes with CNTs led to low-impedance electrodes,<sup>4</sup> and that CNT layers could be used as thin films to enhance or support neuronal excitation.<sup>3–5,9</sup> Chemically modified CNTs are also being used as microelectrode neural interfaces. CNTs can drastically increase the charge injection capacity which can permit the reduction of the electrode size, while providing biocompatible surface and reducing inflammation reaction.<sup>10,11</sup> Lovat et al., by culturing neurons on multi-walled carbon nanotubes substrates,<sup>12</sup> demonstrated that CNTs improved neural signal transfer while supporting dendritic elongation and cell adhesion. These authors observed an increase in the frequency of spontaneous post-synaptic currents and action potential firings, but details of the electrical features of such coupling are still lacking. Indeed, at the cell/CNTs interface, various effects are combined because of the complex and numerous properties of CNTs (conductivity, topography, chemical functionalization, hydrophobicity, and young modulus), but all these phenomena are still not completely understood.

From several studies involving cell culture on CNT layers, it is becoming clear that nanotopography exhibited by CNT layers stimulates behavioral changes in cells and plays a critical role in modifying cell development and proliferation, as well as the strength of adhesion to substrates.<sup>1,2,13</sup> Nano- and microtopography have been recognized as fundamental parameters in the design of bioinspired materials with controlled adhesion.<sup>14,15</sup> However, the results presented in the literature for cell adhesion on nonstructured randomly rough surfaces, which represents the majority of natural surfaces, remain controversial. Some studies have documented a decrease in proliferation and adhesion with the increase in surface roughness,<sup>16</sup> whereas others have shown the opposite by using others cell types.<sup>17</sup> Most of the studies related to the culture of neural cells on CNT substrates used homogeneous surfaces and compared several surface types.<sup>18</sup> However, patterned surfaces are a key design to study and interpret cell surface interactions. Only a few studies have reported experiments using patterned surfaces, for example, to study the cellular anchorage mechanism and the role of the nanoscale neurite–CNT interaction<sup>19–22</sup> or to form engineered, electrically viable networks of neurons.<sup>21</sup> Micropatterning of CNTs using lithography to create self-organizing networks has been demonstrated.<sup>11</sup> Gabay et al. used a polydimethylsiloxane stamp to deposit nanoparticles onto a quartz surface to generate catalytic islands upon which CNTs were grown via chemical vapor deposition.<sup>9</sup> When neurons were cultured onto these patterns, neurons adhered essentially on CNT regions. Sorkin et al.<sup>23</sup> used a similar approach and created patterned networks to study functional neuron networking with CNT discs serving as electrical connections for sensing or stimulation. The patterning approach is thus very useful for the generation and investigation of neural networks in vitro.

However, most of these studies involving CNT patterning used substrates that were initially nonpermissive for cell attachment and growth. These particular conditions could explain the entire selectivity of cells for the CNT regions. In other words, it is the difference in cell attachment on the different surfaces that caused the preferential localization of the cells on CNT patterns. In the present work, we used an original patterning method that combined spray-coating of CNTs and micro-contact printing to create a new configuration for cells, in which they could choose between two permissive surface types: SiO<sub>2</sub> and CNTs. We think that by using this kind of patterned substrate to culture neural cells, we can learn more about many phenomena involved in the interactions between CNTs and neural cells. To explain the observed highest affinity of cells for CNTs, we decided to investigate the adsorption of proteins contained in the cell culture medium to CNT surface. Indeed, several studies have demonstrated the role of nanotopography for protein adsorption.<sup>24</sup> To explore in details the role of CNTs on protein adsorption, we used a quartz-crystal microbalance (QCM). This instrument determines adsorption events on a piezoelectric quartz sensor through the measurement of the mechanical resonance frequency shift due to mass changes.<sup>25,26</sup> By coating the sensing electrode with a thin CNT layer, we could adapt a QCM technique to quantify protein adsorption on this kind of surface and demonstrate a “porous reservoir effect” of CNT surfaces.

## 2. MATERIALS AND METHODS

**2.1. Fabrication of Engineered Substrates for 2D Cell Culture on CNT Patterns.** *Preparation of CNTs Suspensions.* CNTs used in this work were prepared in-house by catalytic chemical vapor deposition (CCVD) of CH<sub>4</sub> at 1000°C (H<sub>2</sub>:CH<sub>4</sub> atmosphere), as reported earlier.<sup>27</sup> After catalyst removal by dissolution with a concentrated aqueous HCl solution, the CNTs were filtered and washed with deionised water (0.45 μm polypropylene filtration membrane) until neutral. The sample contained approximately 80% of the double-walled nanotubes (DWNTs), the rest being mainly single-walled nanotubes (~15%) and triple-walled nanotubes. In order to obtain a stable CNT suspension and to avoid nanotubes agglomeration, we added a noncytotoxic dispersing agent, the carboxymethylcellulose (CMC). DWNTs and CMC were mixed with ultrapure water with a mass ratio of 1:10 (CNTs: 0.1% and CMC: 1%). The CNT concentration of this suspension corresponds to 1 μg/mL. The suspension was sonicated for 30 min (Sonics Vibra Cell) at a power of 150 W, while cooling in an ice bath. The mixture, appearing like a stable black suspension, however, was centrifuged (16 000 rpm for 30 minutes) in order to eliminate the largest agglomerates.

*SiO<sub>2</sub> Substrate Patterning with CNTs using Soft Lithography.* SiO<sub>2</sub> surfaces were patterned with CNTs using an adapted soft lithography method. The first step of this method consisted in inking a microstructured polydimethylsiloxane (PDMS) stamp with CNTs. Details of this process can be found in the Supporting Information. In order to generate dense and homogeneous layers of CNTs on the PDMS stamp surface, we used a spray-coating technique. This technique is cost-effective and scalable to a large area.<sup>28,29</sup> Spray-coating was carried out for 10 min to cover a 2 × 2 cm microstructured PDMS surface and obtain a dense CNT layer, 100 nm in thickness.<sup>30</sup> By controlling the spray-coating duration, it was possible to control the CNT layer thickness. Once the stamp has been covered with a thin CNT layer, it was brought into contact with an ethanol wet SiO<sub>2</sub> surface. The stamp was then peeled away, and we obtained reproducibly largescale patterned SiO<sub>2</sub> surfaces as shown in Figure 1. After fabrication, all surfaces were dipped in a water bath and heated at 60°C for 2 h to remove residual surfactant. We finally obtained micrometric patterns made of CNTs, having a controlled thickness on an SiO<sub>2</sub> surface, and suitable for cell culture experiments. The thin



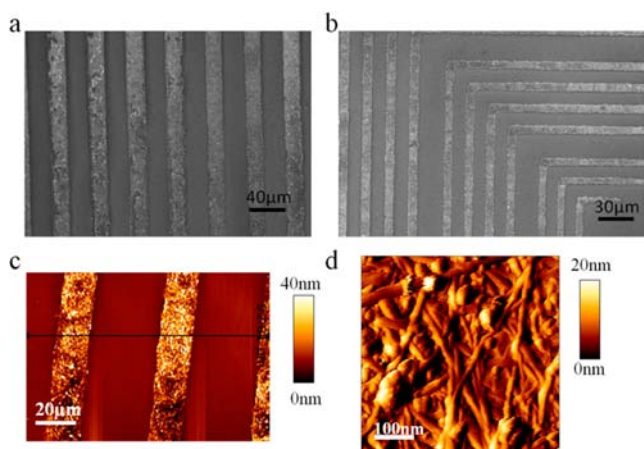


**Figure 1.** Typical surfaces prepared for a 2D cell culture. (a and b) SEM images of a patterned SiO<sub>2</sub> substrate after printing CNTs. The printed features are 7 to 20 μm wide lines. (a) Periodic arrays of line and space CNT arrays. (b) Specific arrays of lines with 90° corners. CNTs appear bright under SEM inspection. (c and d) AFM characterization of typical CNT patterns created by microcontact printing. (c) AFM image of CNT lines on a SiO<sub>2</sub> surface (height signal). (d) AFM image showing details inside a CNT pattern at the nanoscale (vertical deflection signal). There is no CNT ordering inside a micropattern.

layers of CNTs patterned following this  $\mu$ CP process exhibited a metallic behavior. The resistivity is on the order of 0.1  $\Omega$  cm.

This process was applied to create all surfaces used in this work. For surfaces covered with a continuous CNT layer, we used a flat PDMS stamp, while a microstructured PDMS stamp was used to produce patterned surfaces. Two types of patterns were used in this work: the first one consisted of arrays of micrometric lines measuring 20 μm in width and 8 mm in length, and the second one consisted in micrometric lines measuring between 7 μm and 20 μm in width and turning at an angle of 90°. Various DWNT layer thicknesses (between 20 and 100 nm) were used, as mentioned for each experiment. Details of the process can be found in the Supporting Information.

**2.2. Cell Culture.** Neuroblastoma mouse cells (neuro2a) were grown in DMEM medium supplemented with 10% fetal bovine serum (PAA Laboratories) and 1% penicillin streptomycin (GIBCO) in petri dishes. Cells were subcultured twice a week and maintained at 37°C and 5% CO<sub>2</sub>. All reported experiments were performed using cells with less than twenty passages. Neuro2a cells were seeded on substrates at a density of  $1.2 \times 10^4$  cells/cm<sup>2</sup>. Cells were incubated for 24 h and then differentiated by switching the DMEM with 10% serum medium to a medium of DMEM with 1% BSA (bovine serum albumin, Euromedex). Cells were then maintained at 37°C for 48 h before being fixed with 3.5% paraformaldehyde (Sigma) for characterization.

**2.3. Sample Characterization. AFM Measurements.** Atomic force microscopy (NanoWizard II, JPK instruments) was used for imaging CNTs and for measuring the height of CNT layers and the roughness of the patterned surface. All images and measurements were performed in a dry environment at room temperature in contact mode over a sampling of  $50 \times 50 \mu\text{m}^2$  for roughness measurements. Multiple measurements were made in different scan directions. At least three images were recorded per sample. The images had a resolution of  $256 \times 256$  pixels and were acquired at a scanning rate of about 1 Hz.

**SEM Observations.** A scanning electron microscope (SEM) (Hitachi S-4800) was used to characterize both patterned surfaces alone and patterned surfaces with cultured cells to investigate cell and neurite localization. Substrates were rinsed with a phosphate-buffered saline solution, dried, and directly used for SEM observation. For patterned surfaces with cultured cells, quantifications were realized by counting at least 300 cells on four randomly chosen fields (200 $\times$  magnification).

**Fluorescence Microscopy and Image Analysis.** To observe cells and quantify their behavior, the actin cytoskeleton and cell nucleus were stained. Cells were fixed for 1 hour in a 3.7% (wt/vol) solution with formaldehyde, containing 15 mM sucrose at room temperature. After permeabilization with Triton X100, F-actin was stained with tetramethylrhodamine (TRITC)-conjugated phalloidin (molecular probes), at a dilution of 1:200. The cell nucleus was stained with 4'-6-diamidino-2-phenyl indole (DAPI) used in a 1:100 ratio. Fluorescence images were acquired using a Leica fluorescent microscope with a 20 $\times$  objective. Images of at least 300 cells on four randomly chosen observation fields were captured and analyzed for each experimental condition. Experiments have been repeated at least three times. Neuro2a cells were considered as differentiated when they developed at least one neurite measuring at least 20 μm in length.

**Statistical Analysis.** Statistical analysis was based on at least three independent series of experiments. A *t* test or a one-way ANOVA analysis was performed using GraphPad Prism. Statistical significance is indicated as follows: \*\*\**p* < 0.001, \*\**p* < 0.01, and \**p* < 0.05.

**2.4. Quartz Crystal Microbalance Measurements.** For quartz crystal microbalance measurements, we used an E4 quartz crystal microbalance with dissipation monitoring (QCM-D) from Q-Sense. Two separated identical flow chambers were used. One chamber contained virgin SiO<sub>2</sub> quartz, and the second chamber contained SiO<sub>2</sub> quartz covered with a continuous CNT layer. CNT layers of various thicknesses were used. The resonance frequency baseline signal was stabilized before the injection of culture medium elements into the chambers. The 7th resonance frequency was chosen for data analysis. The experiments were conducted at the temperature used to culture neural cells (i.e., 37°C).

A simplified version of the Sauerbrey equation can be used with respect to the type of crystal used in the study. The additional mass per unit area (in ng/cm<sup>2</sup>) is  $\Delta m = -(17.7/n) \times \Delta f$ , where *n* = 7 (7th order) and  $\Delta f$  is the absolute value of the negative resonance frequency shift measured in real time, which gives a variation of 2.53 ng/cm<sup>2</sup> for a  $\Delta f$  of 1 Hz.

**2.5. Effects of CNTs on Neural Cells Proliferation.** Neuro2a cells were cultured in parallel on a plane SiO<sub>2</sub> surface and on a plane SiO<sub>2</sub> surface coated with a homogeneous  $60 \pm 10$  nm thick layer of CNTs, hereafter called a CNT surface. In this case, a pure solution of fetal bovine serum (FBS) was incubated prior to the cell culture on both surfaces for 3 h. After removal of the FBS solution, surfaces were air dried. Cells were seeded on surfaces at an initial density of  $1.2 \times 10^4$  cells/cm<sup>2</sup> and cultured as usual. For a quantitative analysis of proliferation, cell densities were counted each day for 4 days by optical microscopy (5 $\times$  objective) on four randomly chosen fields. Experiments were independently repeated three times.

### 3. RESULTS

The primary aim of the present study was to investigate the effects of CNTs on neural cell development and to elucidate their role in the cell culture process. For this, we first observed cell behavior of cells cultured in parallel on nonpatterned surfaces made of virgin silicon dioxide surfaces (SiO<sub>2</sub>) or consisting of a dense and thin layer of CNTs printed over a SiO<sub>2</sub> surface (SiO<sub>2</sub>/CNTs). CNT layers were made by using a spray-coating technique. In comparison to other coating techniques such as solution casting<sup>31</sup> or dipping,<sup>32</sup> the spray-coating process developed here allowed for denser CNT layers to be obtained in a single step, with a substrate surface totally covered with CNTs (see the Supporting Information). We thus cultured in parallel and in the same conditions neuro2a cells on a SiO<sub>2</sub> surface, a permissive substrate for neuro2a cells (control), or a thin and continuous CNT layer. No supplementary coating of the surfaces was realized. The affinity between cells and surfaces was evaluated by quantifying adherent cell density and cell differentiation after 3 days of culture. As can be seen in Figure 2, on homogeneous surfaces,

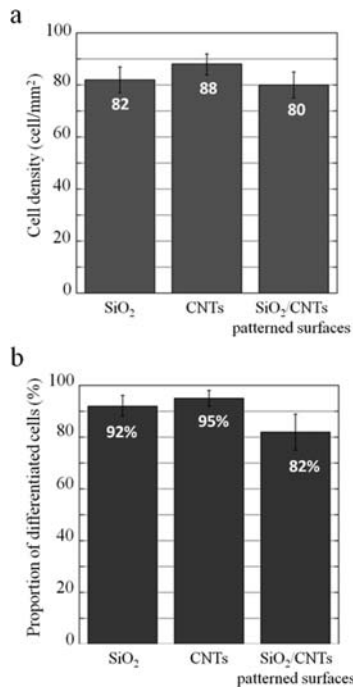


**Figure 2.** Influence of CNTs on neuronal cell (neuro2a) density and differentiation. Neuro2a cells were cultured for 3 days on a SiO<sub>2</sub> nonpatterned surface, on thin nonpatterned layers of CNTs, or on SiO<sub>2</sub>/CNTs line and space patterns. (a) Cell density (DAPI-stained nuclei per mm<sup>2</sup>) on the different surfaces. (b) Percentage of differentiated neural cells (percentage of neuro2a cells exhibiting at least one neurite measuring at least 20 μm) on the different surfaces. Data represent the mean values (± SE) coming from observations of at least 200 cells on four randomly chosen imaging fields obtained for three independent experiments.

these two parameters are comparable regardless of the surface composition. The proportion of differentiated cells raised comparable scores, 92 ± 4% and 95 ± 3%, respectively, for the SiO<sub>2</sub> and CNT surfaces.

We then investigated the influence of CNTs on neural cell morphology, in particular by considering their neurite number. We thus distinguished neural cell populations developing 1 neurite, 2 or 3 neurites, 4 or 5 neurites, and finally 5 or more neurites. Figure 3 shows that when cultured on a SiO<sub>2</sub> surface, a

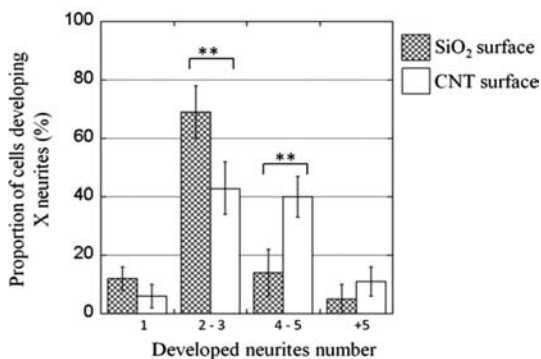


**Figure 3.** Histogram representing the proportion of differentiated neuronal cells equipped with only one neurite, two or three neurites, four or five neurites, or more than five neurites for the two types of unpatterned surfaces: SiO<sub>2</sub> and CNT thin layer. For each condition, around 400 cells were observed.

large majority of cells exhibited only 2 or 3 neurites (69 ± 9%) and that only 14 ± 8% of the neural cells developed 4 or 5 neurites. On the other hand, when cultured on a dense and continuous CNT layer, neural cells globally exhibited more neurites. Namely, the mean neurites number per neuron raised 3.3 ± 0.3 for CNT layer against only 2.2 ± 0.3 neurites per neuron for the SiO<sub>2</sub> surfaces. The proportion of neural cells exhibiting 4 or 5 neurites raised 40 ± 7%, whereas the proportion of neural cells with 2 or 3 neurites was only 43 ± 9% (against 69 ± 9% on virgin SiO<sub>2</sub>, *p* = 0.005). No significant effect was observed concerning the neurites length (data not shown).

Both surface types exhibited equivalent affinity for neuro2a neural cells in term of cell adhesion and differentiation. However, major differences were observed in the developed neurites number. To further investigate the interactions between neural cells and CNTs, we decided to culture those cells in the presence of both surface types by means of patterned surfaces, closely juxtaposing the SiO<sub>2</sub> areas and CNT areas. To create a competition situation between CNTs and SiO<sub>2</sub>, we cultured neural cells on SiO<sub>2</sub> surfaces, patterned through a simple and rapid printing process previously developed. The developed method allowed us to very rapidly process large scale surfaces, thus giving the opportunity to study cell behavior over a large population. Moreover, in contrast with some already described methods,<sup>2,11,33,34</sup> this simple soft lithography process is particularly compatible with the cell culture, as no toxic solvents were used at any step, surfaces could easily be sterilized before starting the cell culture, and CNT patterns were not removed during the whole culture process without any previous chemical functionalization needed.

The patterned surfaces thus obtained were in the plane configuration of CNTs. Directly after cell seeding, cells were randomly distributed and covered the entire surface homogeneously, independent of the presence of the CNT patterns (see the Supporting information). After three days of culturing, the overall cell density and differentiation rate were comparable to those obtained on nonpatterned substrates, as is shown in Figure 2 (panels a and b). We obtained, namely, a cell density of 80 cells/mm<sup>2</sup> and a global differentiation score of 82 ± 7% for SiO<sub>2</sub>/CNT patterned surfaces. But surprisingly, by looking further in depth, we observed that a huge majority of cells developed precisely on the CNT patterns, as illustrated in Figure 4. Moreover, we observed that the neurites were guided in the direction of the printed CNT patterns. Neurites developed and extended in the direction of the CNT lines and were even able to follow lines exhibiting a corner of 90°, as shown in Figure 4.

SEM observations have been complemented by optical fluorescent imagery, and quantitative analyses are presented in Figure 5. In fact, 84 ± 5% of cells were found on CNT patterns in a competition situation (Figure 5a) and cells located on CNT patterns exhibited a higher differentiation rate than cells located on the neighboring SiO<sub>2</sub> areas (Figure 5b). A proportion of the differentiated cells raised 86 ± 4% for cells located on CNT patterns. For cells grown on SiO<sub>2</sub> nearby zones, this score is only of 55 ± 4%, whereas 92 ± 4% of cells were found to be differentiated on a homogeneous SiO<sub>2</sub> surface (see Figure 2b). This observation underlined that cells behaved differently with the proximity of CNT features.

In a second step, we investigated the influence of cell body localization on neurite behavior. For this, we distinguished the

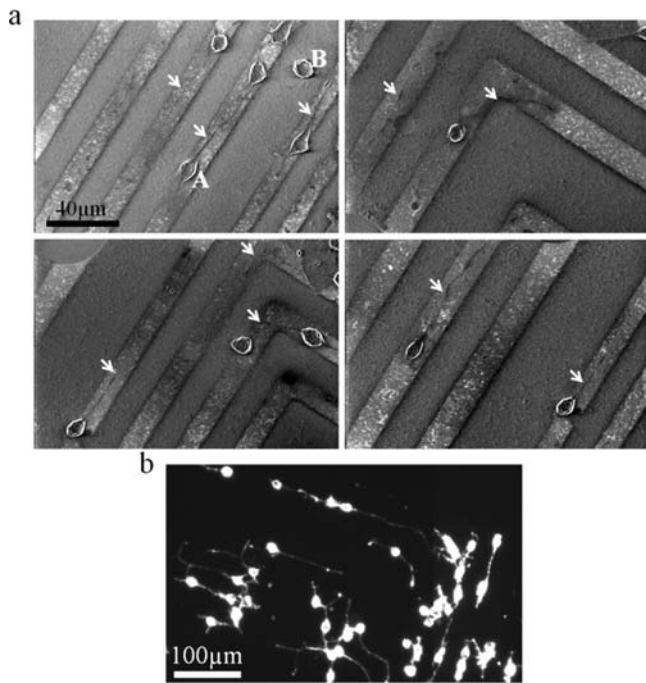


**Figure 4.** Neuro2a cells culture on a SiO<sub>2</sub>/CNTs micropatterned surface. (a) SEM images of neuro2a cells cultured on patterned surfaces after 2 days of differentiation. Arrows point to neurites developed on CNT patterns. The letter A indicates a specific cell body on a CNT feature, and the letter B points out a specific cell body outside of a CNT feature (on a SiO<sub>2</sub> feature). (b) Optical fluorescence image of neural cells grown on CNT patterns (similar to Figure 1, right) after phalloidin staining. Note that neurites follow the CNT lines turning at an angle of 90°.

cell population with the cell body located on the CNT features (denoted “A” in Figure 4a) from cells with bodies located on the SiO<sub>2</sub> features (denoted “B” in Figure 4a). For cells having their body located on the CNT features (population A), 85 ± 5% of their neurites were located on the CNT features as well. Only 15 ± 5% of neurites escaped CNT features to grow on neighboring SiO<sub>2</sub> areas. On the other hand, for cells having their body on SiO<sub>2</sub> features, 54 ± 3% of neurites developed on SiO<sub>2</sub> and other neurites reached a neighboring CNT feature and grew further along it (see Figure 5, panels c and d).

All these observations lead to the conclusion that in the presence of these two kinds of surfaces (SiO<sub>2</sub> and CNTs) close together, the neural cells, neuro2a, preferentially developed on the CNT lines. One possible hypothesis for the selective localization of cells on the CNT patterns is the higher affinity of CNTs for the proteins of the culture medium compared to SiO<sub>2</sub>, thus creating a more favorable environment for cell growth and neurite development. To investigate the possible interaction between proteins of the culture medium and CNTs, we performed QCM-D analysis of adsorption of various elements such as BSA and serum (FBS).

To investigate the precise role of the CNT layer on this phenomenon, QCM-D experiments were carried out using virgin SiO<sub>2</sub> quartz crystals and various SiO<sub>2</sub> quartz coated with continuous CNT layers of different thicknesses. All CNT layers were first characterized by AFM. They had a comparable surface roughness ( $R_a = 8.5 \pm 2$  nm) and measured between 20 and 100 nm in height. Bovine serum albumin (BSA), at a concentration of 10 µg/mL, was then incubated on both quartz crystal types. In our cell culture experiments, BSA was used at

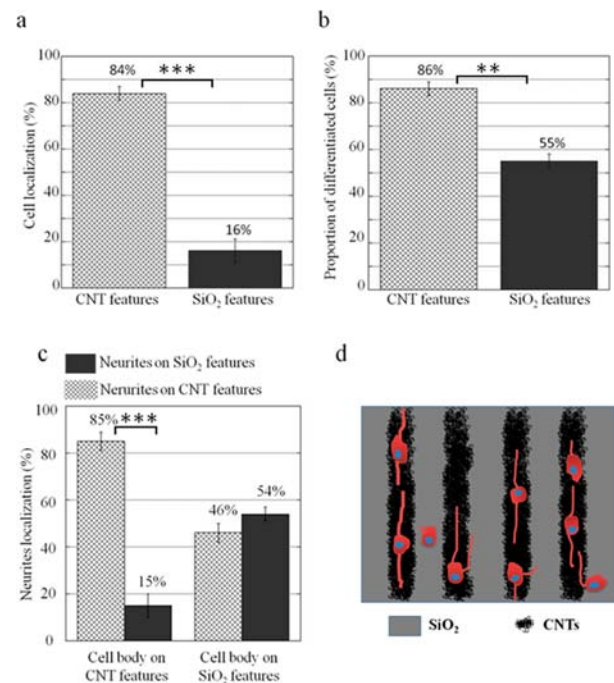


**Figure 5.** Influence of SiO<sub>2</sub>/CNTs micropatterns on neuro2a cell behavior. (a) Detailed distribution of cells inside a SiO<sub>2</sub>/CNT pattern (18 µm line and 22 µm space). (b) Detailed differentiation scores of cells inside a SiO<sub>2</sub>/CNT pattern. (c and d) Detailed neurite outgrowth on patterned surfaces. (c) Quantification of neurite localization inside SiO<sub>2</sub>/CNT patterns, as a function of the localization of the cell body. Values represent mean (± SE) of three independent experiments. At least 300 neurites were observed for each experiment. (d) Schematic representation of various situations observed for neural cell culture on the SiO<sub>2</sub>/CNT patterned surfaces (CNTs are shown in black). Cell bodies are mainly located on the CNT patterns. Neurites turned out to develop preferentially on CNT patterns and followed the direction of the CNT lines. Cells located on SiO<sub>2</sub> developed less neurites, which were either localized on the SiO<sub>2</sub> regions or on the CNT patterns and aligned by the CNT lines.

this concentration to induce neural cell differentiation. Figure 6a shows typical QCM traces obtained when incubating substrates with BSA. As soon as BSA entered the chambers, a frequency shift was detected, denoting adsorption events on both surfaces. This frequency shift was always significantly greater for the quartz covered with CNTs. Thus, we observed a clear and reproducible difference between the two surface types (SiO<sub>2</sub> and CNTs). Namely, CNT surfaces exhibiting higher frequency shifts adsorbed more BSA than virgin SiO<sub>2</sub> quartz.

Frequency shift (and thus mass adsorption) was found to be directly linked with the CNT layer thickness (Figure 6, panels a and b). For a layer thickness between 20 and 70 nm, we noted a proportional relation between the adsorbed mass of proteins and the layer thickness (correlation factor is 0.98) (Figure 6b). However, for layers thicker than 70 nm, the adsorbed mass did not increase any more, as if the layers were saturated and could not adsorb additional proteins. After incubation of BSA on both surface types, we washed the quartz with PBS in order to know if BSA proteins were strongly attached to the surface. We observed a low desorption of BSA for both surface types (see the Supporting Information). However, the washing process only removed loosely attached proteins, and a significant amount of BSA proteins remained adsorbed on the surfaces. Once again, the amount of BSA proteins found on the surface



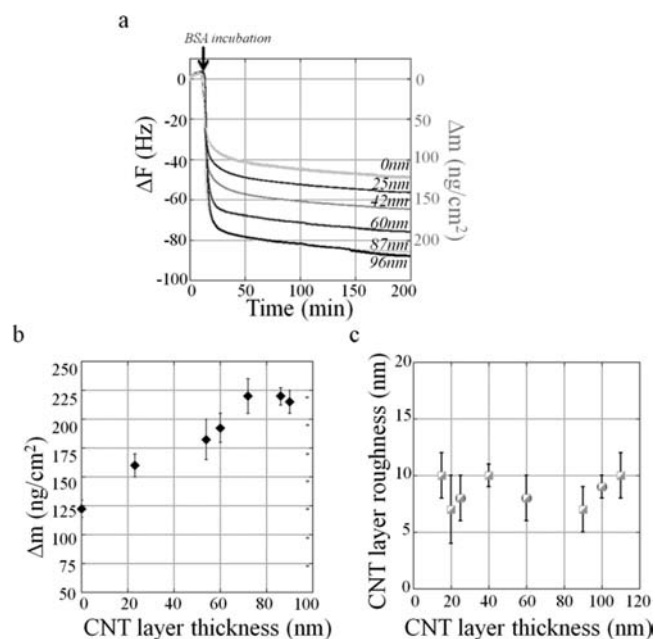


**Figure 6.** QCM-D investigation of BSA adsorption on unpatterned CNT thin layers of increasing thickness, printed on a SiO<sub>2</sub> surface. (a) Typical QCM-D frequency responses to the incubation of a BSA solution (10 μg/mL diluted in PBS) for virgin SiO<sub>2</sub> quartz (light blue curve) and for SiO<sub>2</sub> quartz covered with continuous CNT layers of various heights. BSA was introduced at  $t = 9$  min following a baseline preincubation with PBS/BSA-free solution. The curves display the 7th resonance frequency shift, and the corresponding surface density of adsorbed mass is displayed on the right vertical axis. (b) Evolution of the final frequency shift (after 200 minutes of incubation) measured by QCM-D. (c) Evolution of the CNT layer roughness against the thickness of the CNT layer measured by AFM.

after incubation and rinsing was significantly higher on the CNT surfaces compared to the SiO<sub>2</sub> surfaces (see Figure S1 of the Supporting Information).

In order to confirm the increasing adsorption on the CNTs, we carried out the same experiments with other molecules, such as poly-L-lysine, which is very often used to enhance cell adhesion and fetal bovine serum, which is commonly added to the cell culture medium or an antibody (donkey-anti-goat IgG monoclonal antibody). Table 1 summarizes the obtained

**Table 1. Relative Frequency Shifts Measured After the Incubation (200 minutes) of Various Solutions<sup>a</sup>**

entity	$\Delta F$ CNTs/ $\Delta F$ SiO <sub>2</sub>
BSA (10 μg/mL)	1.3
poly-L-lysine (40 μg/mL)	4
foetal bovine serum	1.6
antibody (40 μg/mL)	4.3

<sup>a</sup>The ratio represents the final frequency shift measured by QCM-D on a CNT thin layer (layer thickness is  $80 \pm 5$  nm) printed on a SiO<sub>2</sub> quartz, divided by the same quantity measured on a virgin SiO<sub>2</sub> quartz.

results. We always observed that the amount of molecules adsorbed on the CNT surfaces was significantly higher than on the SiO<sub>2</sub> surfaces, whatever the incubated solution. The frequency shift difference between SiO<sub>2</sub> and CNT surfaces was particularly high for antibodies and poly-L-lysine (around 4 times higher).

In order to illustrate the enhanced adsorption of CNTs and investigate its effect on the cell culture, we compared cell proliferation on both CNT and SiO<sub>2</sub> surfaces. For this specific investigation, both surfaces were used either uncoated or coated with fetal bovine serum. Figure 7 represents proliferation curves

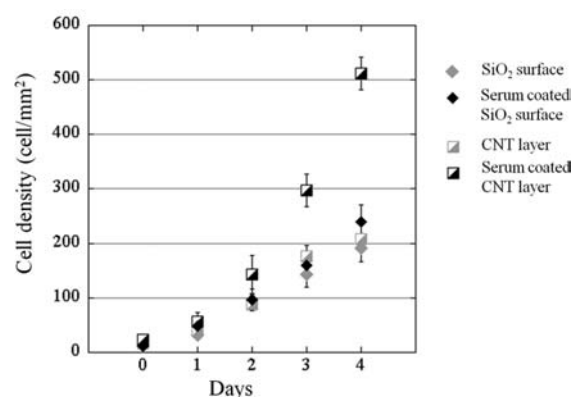


**Figure 7.** Cell density curves for neuro2a cells on SiO<sub>2</sub>, SiO<sub>2</sub> coated with fetal bovine serum, CNT layers (layer thickness is  $80 \pm 5$  nm), and CNT layers coated with fetal bovine serum. Each data point is the average cell density from three experiments. Error bars indicate the standard error (SE).

obtained for those four surfaces after 4 day long cultures. We clearly observed that proliferation was accelerated on the coated CNT surface in comparison with the uncoated CNT surface. After 4 days of culture, the cell number on the coated CNT surface was more than twice higher (2.4) than on all other surfaces. The same coating realized on SiO<sub>2</sub> did not lead to comparable increasing proliferation, underlying that CNTs adsorbed a higher quantity of FBS are responsible for this high proliferation rate.

#### 4. DISCUSSION

In the first step, we noted that CNTs drastically increased the average number of neurites per cell. The number of cells equipped with 4 or 5 neurites was three times higher on CNTs than on a SiO<sub>2</sub> surface. Studies performed using as-produced CNTs did not always show similar results. For example, Mattson et al.<sup>13</sup> found that surfaces of unmodified nanotubes were favorable for neurites outgrowth but did not promote neurite branching, suggesting that adhesion of growth cones to the carbon surface was relatively weak. In contrast, neurons grown on CNTs coated with a bioactive molecule, such as 4-hydroxynonenal<sup>13</sup> or nerve growth factors,<sup>35</sup> elaborate multiple neurites, which exhibit extensive branching. Matsumoto et al.<sup>35</sup> showed that CNTs coated with NGF promoted neurite outgrowths in the same manner as soluble NGF. Hu et al.<sup>2</sup> showed that multiwalled carbon nanotubes (MWNTs) were also a permissive substrate for rat hippocampal neurons. In this study, the authors showed that both polyethyleneimine and as-prepared MWNTs supported neuronal viability and permitted neurite outgrowth. However, as-produced MWNTs were found to reduce the initiation of neurite outgrowth, characterized by the reduction of the growth cone number and the neurite number per neuron. The studies discussed above focused on investigating CNT–neuron interactions by varying the surface chemistry of CNT substrates. Mechanical and electrical properties of CNT substrates such as surface roughness and conductivity, respectively, could also modulate and increase

neuronal growth and neurite outgrowth.<sup>19,21,36</sup> In our case, CNTs were used as-produced, and no supplementary coating was performed previous to the cell culture. CNT layers exhibited a higher roughness than the SiO<sub>2</sub> surface, which could partially explain the increased neurites number we obtained, compared to our control surface.

By patterning, we created a situation in which cells have the choice to develop either on SiO<sub>2</sub> features or on CNT features. This original experimental design turned out to reveal new effects that could not be anticipated from cell culture experiments achieved on nonpatterned surfaces. Cell culture results on those patterned surfaces showed, firstly, that the global adherent cell number was comparable to the scores obtained for nonpatterned surfaces. However, some selectivity of the CNT features was observed, and cells were found to develop preferentially on the CNT features. Directly after cell seeding, cells were randomly distributed (see the Supporting Information). However, during the first day of the culture, cells had migrated, and cell spreading was observed preferentially on CNT features. This means that the cells were able to explore their neighboring environment. Most of the cells were located on CNT features and exhibited a higher differentiation rate compared to residual cells growing on SiO<sub>2</sub> neighboring areas, which were not able to spread and migrate enough for joining adjacent CNT features. In conclusion, our investigation of patterned CNT/SiO<sub>2</sub> surfaces revealed that CNTs appeared to be more attractive for cell adhesion, growth, and differentiation.

In the same way, we have observed that neurites were guided by the CNT patterns. Neurites elongated along patterned CNT lines. Even for the CNT patterns lines turning at an angle of 90°, neurites followed pattern geometry. This indicated that the attractive effect of CNTs happened at two different length scales: firstly, at the cell body scale, explaining cell localization selectivity and secondly, at the neurite scale, during growth. Those guiding effects of CNT features suggest that neurites were confronted with the same choice of cell body. They explored their local environment and finally grew on the most favorable surface. This explanation is further supported by the fact that even cells which were not able to develop on CNTs very often exhibited neurites on the CNT patterns. One origin of this selective effect could be that the CNT features exhibited a higher surface roughness than the neighboring SiO<sub>2</sub> features, as was often mentioned in the literature.<sup>37,38,17</sup> This effect of CNTs on neuronal adhesion, for example, was explored in a recent study by Sorkin et al.,<sup>19</sup> who cultured neurons from embryonic rat cortices on CNT features that consisted of micrometric discs. Cells displayed a preference to grow on CNT discs, and a close examination revealed extensive curling of the neurites around CNTs. The authors explained that CNT discs allowed entanglement of thin neurites with relatively similar diameters to CNTs, and that such an entanglement may represent an anchoring mechanism allowing neurons to attach to rough surfaces. Gentile et al.<sup>17</sup> recently reported that cells preferentially grow on etched silicon rough surfaces. An increased proliferation rate was obtained for moderately rough surfaces (Ra: ~10–45 nm). According to them, this could be attributed to several possible mechanisms, among which is the increased effective surface energy over nonplanar substrates. Cell stable adhesion and consequent proliferation would be energetically favorable on rough surfaces. Therefore, the theory of adhesion of elastic solids (here the cells) on randomly rough surfaces could explain the observed preferential stable adhesion and cell localization.<sup>17,39</sup> Furthermore, a

rough surface allowed a higher number of possibilities for cells to construct adhesion complexes with the surface.<sup>14,17,40</sup>

The processes that mediate the cellular adhesion to nanoscale surface structures are, however, not well understood and may be a direct result of the influence of the surface topography/roughness, as discussed above, or an indirect one. Our results showed that CNT features could act as porous reservoirs for various elements (proteins, growth factors, etc.) contained in the culture medium. Once again, this latter effect may originate from the enhanced roughness of the CNT surfaces. These results are in accordance with Chung et al.,<sup>41</sup> who found that quartz electrodes equipped with CNTs had an increased specific surface area, leading to enhanced adsorption of chitosan. However, we showed that protein adsorption was affected by the CNT layer thickness (see Figure 6b). By increasing the CNT layer thickness exhibiting the same surface roughness (see Figure 6c), we increased protein adsorption. We were even able to evidence a linear relation between CNT layer thickness and adsorbed protein mass. However, this phenomenon seemed to be limited by protein diffusion inside the CNT network. Indeed, for CNT layer thickness above 70 nm, proteins could not diffuse deeper in the CNT network, leading to a kind of saturation. The same observations were made for various types of proteins. This result clearly shows that the enhancement of protein adsorption on the CNT layers is dominated by a bulk effect rather than a pure surface effect. Indeed, different layers of the same surface roughness exhibited increased adsorption with increasing thickness. Thus, we think that the dominant effect responsible for this enhanced protein adsorption is the generation of a porous network of nanoscale elements acting as a reservoir of proteins rather than a pure roughness induced effect. Finally, we have shown that the CNT layers could be charged with proteins and that cells, in the presence of CNT patterns, could be able to sense a surface concentration gradient. This surface gradient on patterned substrates could explain why cells chose to grow preferentially on CNT features, taking advantage of the numerous proteins adsorbed on the CNT patterns. This interpretation is further supported by our observation that cells duplicated more rapidly when CNT layers were charged with serum previously to the cell culture. Previous reports on how surface topography or roughness affect protein adsorption are numerous, see ref 42, for example. Dynamic interactions between nanotopography and proteins are complex, due to the combination of attractive and repulsive forces which are governed by local changes in surface properties.<sup>43–45</sup> The overall effect of surface nanoscale features is not fully understood, according to reports available in the literature.<sup>42,46,47</sup> In our case, CNT surfaces always lead to an increased mass adsorption with various ranges of proteins, as antibodies or bovine serum albumin, suggesting that the CNT patterns could act as local porous reservoirs for active proteins of the culture medium. This could explain all of our results obtained on the cell culture.

## 5. CONCLUSION

Patterning SiO<sub>2</sub> surfaces with CNTs created a new original situation for cell culture experiments and revealed new phenomena on cell interactions with CNTs. We have evidenced that CNTs enhanced protein adsorption, leading to protein gradients on the patterned surface. Patterned substrates thus exhibited two types of surfaces that are different in terms of composition, roughness, and protein amount. Our results show that neural cells preferentially adhere to the CNT patterns.



CNTs thus appear to be the most convenient surface for cell growth and differentiation, in comparison with the SiO<sub>2</sub> surface. This conclusion could not be obtained by culturing cells on homogeneous surface types consisting either of CNTs or of SiO<sub>2</sub>. Namely, cells were able to adapt to SiO<sub>2</sub> and exhibited comparable adhesion and development on SiO<sub>2</sub> and on CNTs. Finally, this shows that patterning can be useful to determine the most appropriate growth surface for cells. It would be interesting to investigate the distance over which cells are able to migrate in order to grow on a neighbouring appropriate CNT surface. Thus, we could obtain information on the balance between cell mobility and surface attraction. Among the possible mechanisms capable to explain the preferential adhesion, differentiation, and growth of neural cells on CNT patterns, this paper highlights the existence of an indirect cell/CNT interaction mediated by the preferential adsorption of culture medium proteins on CNT networks.

## ■ ASSOCIATED CONTENT

### ● Supporting Information

The fabrication process of CNT micropatterned surfaces and typical QCM-D responses to BSA solution incubation are detailed in a supporting pdf file. This material is available free of charge via the Internet at <http://pubs.acs.org>.

## ■ AUTHOR INFORMATION

### Corresponding Author

\*E-mail: [abeduer@laas.fr](mailto:abeduer@laas.fr). Tel: +33 5 61 33 63 75. Fax: +33 5 61 33 62 08. Address: LAAS-CNRS Amélie Bédurier, Groupe NBS, 7 Avenue du Colonel Roche, 31077 Toulouse Cedex 4, France.

### Notes

The authors declare no competing financial interest.

## ■ ACKNOWLEDGMENTS

The authors acknowledge the technical staff of the clean room facility of LAAS-CNRS for their assistance in silicon master fabrication for the micro-contact printing process.

## ■ REFERENCES

- (1) Hu, H.; Ni, Y.; Mandal, S. K.; Montana, V.; Zhao, B.; Haddon, R. C.; Parpura, V. Polyethyleneimine functionalized single-walled carbon nanotubes as a substrate for neuronal growth. *J. Phys. Chem. B* **2005**, *109*, 4285–4289.
- (2) Hu, H.; Ni, Y.; Montana, V.; Haddon, R. C.; Parpura, V. Chemically functionalized carbon nanotubes as substrates for neuronal growth. *Nano Lett.* **2004**, *4*, 507–511.
- (3) Webster, T. J.; Waid, M. C.; McKenzie, J. L.; Price, R. L.; Ejiogor, J. U. Nano-biotechnology: Carbon nanofibres as improved neural and orthopaedic implants. *Nanotechnology* **2004**, *15*, 48–54.
- (4) Keefer, E. W.; Botterman, B. R.; Romero, M. I.; Rossi, A. F.; Gross, G. W. Carbon nanotube coating improves neuronal recordings. *Nat. Nanotechnol.* **2008**, *3*, 434–439.
- (5) Lee, H. J.; Park, J.; Yoon, O. J.; Kim, H. W.; Lee, D. Y.; Kim, D. H.; Lee, W. B.; Lee, N.; Bonventre, J. V.; Kim, S. S. Amine-modified single-walled carbon nanotubes protect neurons from injury in a rat stroke model. *Nat. Nanotechnol.* **2011**, *6*, 121–125.
- (6) Smart, S.; Cassidy, A.; Lu, G.; Martin, D. The biocompatibility of carbon nanotubes. *Carbon* **2006**, *44*, 1034–1047.
- (7) Shein, M.; Greenbaum, A.; Gabay, T.; Sorkin, R.; David-Pur, M.; Ben-Jacob, E.; Hanein, Y. Engineered neuronal circuits shaped and interfaced with carbon nanotube microelectrode arrays. *Biomed. Microdevices* **2008**, *11*, 495–501.
- (8) Gheith, M.; Pappas, T.; Liopo, A.; Sinani, V.; Shim, B.; Motamedi, M.; Wicksted, J.; Kotov, N. Stimulation of neural cells by lateral currents in conductive layer-by-layer films of single-walled carbon nanotubes. *Adv. Mater.* **2006**, *18*, 2975–2979.
- (9) Fabro, A.; Villari, A.; Laishram, J.; Scaini, D.; Toma, F. M.; Turco, A.; Prato, M.; Ballerini, L. Spinal cord explants use carbon nanotube interfaces to enhance neurite outgrowth and to fortify synaptic inputs. *ACS Nano* **2012**, *6*, 2041–2055.
- (10) Gabay, T.; Ben-David, M.; Kalifa, I.; Sorkin, R.; Abrams, Z. R.; Ben-Jacob, E.; Hanein, Y. Electro-chemical and biological properties of carbon nanotube based multi-electrode arrays. *Nanotechnology* **2007**, *18*, 035201.
- (11) Jakobs, E.; Ben-Jacob, E.; Hanein, Y.; Gabay, T. Engineered self-organization of neural networks using carbon nanotube clusters. *Phys A (Amsterdam, Neth.)* **2005**, *350*, 611–621.
- (12) Lovat, V.; Pantarotto, D.; Lagostena, L.; Cacciari, B.; Grandolfo, M.; Righi, M.; Spalluto, G.; Prato, M.; Ballerini, L. Carbon nanotube substrates boost neuronal electrical signaling. *Nano Lett.* **2005**, *5*, 1107–1110.
- (13) Mattson, M. P.; Haddon, R. C.; Rao, A. M. Molecular functionalization of carbon nanotubes and use as substrates for neuronal growth. *The Journal of Mathematical Neuroscience* **2000**, *14*, 175–182.
- (14) Brunetti, V.; Maiorano, G.; Rizzello, L.; Sorce, B.; Sabella, S.; Cingolani, R.; Pompa, P. P. Neurons sense nanoscale roughness with nanometer sensitivity. *Proc. Natl. Acad. Sci. U.S.A.* **2010**, *107*, 6264–6269.
- (15) Bédurier, A.; Vieu, C.; Arnauduc, F.; Sol, J. C.; Loubinoux, I.; Vaysse, L. Engineering of adult human neural stem cells differentiation through surface micropatterning. *Biomaterials* **2012**, *33*, 504–514.
- (16) Kunzler, T. P.; Huwiler, C.; Drobek, T.; Vörös, J.; Spencer, N. D. Systematic study of osteoblast response to nanotopography by means of nanoparticle-density gradients. *Biomaterials* **2007**, *28*, 5000–5006.
- (17) Gentile, F.; Tirinato, L.; Battista, E.; Causa, F.; Liberale, C.; Di Fabrizio, E. M.; Decuzzi, P. Cells preferentially grow on rough substrates. *Biomaterials* **2010**, *31*, 7205–7212.
- (18) Agarwal, S.; Zhou, X.; Ye, F.; He, Q.; Chen, G. C. K.; Soo, J.; Boey, F.; Zhang, H.; Chen, P. Interfacing live cells with nanocarbon substrates. *Langmuir* **2010**, *26*, 2244–2247.
- (19) Sorkin, R.; Greenbaum, A.; David-Pur, M.; Anava, S.; Ayali, A.; Ben-Jacob, E.; Hanein, Y. Process entanglement as a neuronal anchorage mechanism to rough surfaces. *Nanotechnology* **2009**, *20*, 015101.
- (20) Abdullah, C. A. C.; Asanithi, P.; Brunner, E. W.; Jurewicz, I.; Bo, C.; Azad, C. L.; Ovalle-Robles, R.; Fang, S.; Lima, M. D.; Lepro, X.; Collins, S.; Baughman, R. H.; Sear, R. P.; Dalton, A. B. Aligned, isotropic and patterned carbon nanotube substrates that control the growth and alignment of chinese hamster ovary cells. *Nanotechnology* **2011**, *22*, 205102.
- (21) Zhang, X.; Prasad, S.; Niyogi, S.; Morgan, A.; Ozkan, M.; Ozkan, C. S. Guided neurite growth on patterned carbon nanotubes. *Sens. Actuators, B* **2005**, *106*, 843–850.
- (22) Malarkey, E. B.; Parpura, V. Carbon nanotubes in neuroscience. *Acta Neurochirurgica Supplement* **2010**, *106*, 337–341.
- (23) Sorkin, R.; Gabay, T.; Blinder, P.; Baranes, D.; Ben-Jacob, E.; Hanein, Y. Compact self-wiring in cultured neural networks. *Journal of Neural Engineering* **2006**, *3*, 95–101.
- (24) Kotov, N. A.; Winter, J. O.; Clements, I. P.; Jan, E.; Timko, B. P.; Campidelli, S.; Pathak, S.; Mazzatenta, A.; Lieber, C. M.; Prato, M.; Bellamkonda, R. V.; Silva, G. A.; Kam, N. W. S.; Patolsky, F.; Ballerini, C. I. Nanomaterials for neural interfaces. *Adv. Mater.* **2009**, *21*, 3970–4004.
- (25) Kanazawa, K. K.; Gordon, J. G. Frequency of a quartz microbalance in contact with liquid. *Anal. Chem.* **1985**, *57*, 1770–1771.
- (26) Cooper, M. A.; Singleton, V. T. A survey of the 2001 to 2005 quartz crystal microbalance biosensor literature: Applications of

- acoustic physics to the analysis of biomolecular interactions. *J. Mol. Recognit.* **2007**, *20*, 154–184.
- (27) Flahaut, E.; Bacsá, R.; Peigney, A.; Laurent, C. Gram-scale CCVD synthesis of double-walled carbon nanotubes. *Chem. Commun.* **2003**, *12*, 1442–1443.
- (28) Majumder, M.; Rendall, C.; Li, M.; Behabtu, N.; Eukel, J. A.; Hauge, R. H.; Schmidt, H. K.; Pasquali, M. Insights into the physics of spray coating of SWNT films. *Chem. Eng. Sci.* **2010**, *65*, 2000–2008.
- (29) Bédúer, A.; Vaysse, L.; Flahaut, E.; Seichepine, F.; Loubinoux, L.; Vieu, C. Multi-scale engineering for neuronal cell growth and differentiation. *Microelectron. Eng.* **2011**, *88*, 1668–1671.
- (30) Bédúer, A.; Seichepine, F.; Flahaut, E.; Vieu, C. A simple and versatile micor contact printing method for generating carbon nanotubes patterns on various substrates. *Microelectron. Eng.* **2012**, *97*, 301–305.
- (31) Meitl, M. A.; Zhou, Y.; Gaur, A.; Jeon, S.; Usrey, M. L.; Strano, M. S.; Rogers, J. A. Solution casting and transfer printing single-walled carbon nanotube films. *Nano Lett.* **2004**, *4*, 1643–1647.
- (32) Rahy, A.; Bajaj, P.; Musselman, I. H.; Hong, S. H.; Sun, Y.; Yang, D. J. Coating of carbon nanotubes on flexible substrate and its adhesion study. *Appl. Surf. Sci.* **2009**, *255*, 7084–7089.
- (33) Jang, M. J.; Namgung, S.; Hong, S.; Nam, Y. Directional neurite growth using carbon nanotube patterned substrates as a biomimetic cue. *Nanotechnology* **2010**, *21*, 235102.
- (34) Park, S.; Namgung, S.; Kim, B.; Im, J.; Kim, J.; Sun, K.; Lee, K.; Nam, J.; Park, Y.; Hong, S. Carbon nanotube monolayer patterns for directed growth of mesenchymal stem cells. *Adv. Mater.* **2007**, *19*, 2530–2534.
- (35) Matsumoto, K.; Sato, C.; Naka, Y.; Kitazawa, A.; Whitby, R. L. D.; Shimizu, N. Neurite outgrowths of neurons with neurotrophin-coated carbon nanotubes. *J. Biosci. Bioeng.* **2007**, *103*, 216–220.
- (36) Malarkey, E. B.; Fisher, K. A.; Bekyarova, E.; Liu, W.; Haddon, R. C.; Parpura, V. Conductive single-walled carbon nanotube substrates modulate neuronal growth. *Nano Lett.* **2009**, *9*, 264–268.
- (37) Biggs, M. J. P.; Richards, R. G.; Dalby, M. J. Nanotopographical modification: A regulator of cellular function through focal adhesions. *Nanomedicine: Nanotechnology, Biology, and Medicine* **2010**, *6*, 619–633.
- (38) Voge, C. M.; Stegemann, J. P. Carbon nanotubes in neural interfacing applications. *Journal of Neural Engineering* **2011**, *8*, 011001.
- (39) Persson, B. N. J. Adhesion between an elastic body and a randomly rough hard surface. *Eur. Phys. J. E: Soft Matter Biol. Phys.* **2002**, *8*, 385–401.
- (40) Gittens, R. A.; McLachlan, T.; Olivares-Navarrete, R.; Cai, Y.; Berner, S.; Tannenbaum, R.; Schwartz, Z.; Sandhage, K. H.; Boyan, B. D. The effects of combined micron-/submicron-scale surface roughness and nanoscale features on cell proliferation and differentiation. *Biomaterials* **2011**, *32*, 3395–3403.
- (41) Chung, T.; Limpanichpakdee, T.; Yang, M.; Tyan, Y. An electrode of quartz crystal microbalance decorated with CNT/chitosan/fibronectin for investigating early adhesion and deforming morphology of rat mesenchymal stem cells. *Carbohydr. Polym.* **2011**, *85*, 726–732.
- (42) Lord, M. S.; Foss, M.; Besenbacher, F. Influence of nanoscale surface topography on protein adsorption and cellular response. *Nano Today* **2010**, *5*, 66–78.
- (43) Roach, P.; Eglín, D.; Rohde, K.; Perry, C. C. Modern biomaterials: A review—bulk properties and implications of surface modifications. *J. Mater. Sci.: Mater. Med.* **2007**, *18*, 1263–1277.
- (44) Wilson, C. J.; Clegg, R. E.; Leavesley, D. I.; Percy, M. J. Mediation of biomaterial-cell interactions by adsorbed proteins: A review. *Tissue Eng.* **2005**, *11*, 1–18.
- (45) Woo, K. M.; Chen, V. J.; Ma, P. X. Nano-fibrous scaffolding architecture selectively enhances protein adsorption contributing to cell attachment. *J. Biomed. Mater. Res., Part A* **2003**, *67*, 531–537.
- (46) Shen, J.; Wu, T.; Wang, Q.; Kang, Y. Induced stepwise conformational change of human serum albumin on carbon nanotube surfaces. *Biomaterials* **2008**, *29*, 3847–3855.
- (47) Rechendorff, K.; Hovgaard, M. B.; Foss, M.; Zhdanov, V. P.; Besenbacher, F. Enhancement of protein adsorption induced by surface roughness. *Langmuir* **2006**, *22*, 10885–10888.